Studies of the Kinetics of Two Parallel Reactions: Ammonia Decomposition and Nitriding of Iron Catalyst

Walerian Arabczyk and Rafat Pelka*

Szczecin University of Technology, Institute of Chemical and Environment Engineering, Puaskiego 10, 70-322 Szczecin, Poland

Received: September 8, 2008; Revised Manuscript Received: October 27, 2008

The reaction of ammonia decomposition and nitriding reaction as an example of the parallel reactions were studied. A surface reaction was assumed as the rate limiting step. The experiments were carried out in the range of temperatures from 623 to 723 K. Mixtures of different iron nitrides (γ'-Fe_4N, ϵ-$Fe_{3-2}N$) were obtained. Differential tubular reactor with thermogravimetric (TG) measurement and analysis of the gas phase composition in the reaction volume was used. Reacting gases flowing through the reactor were mixed. Effective reactor volume was determined. The rate constants for ammonia decomposition and ammonia adsorption process at critical point between α-Fe and γ'-Fe_4N phases were estimated. The number of collisions and the sticking coefficient of ammonia over α-Fe phase were also assessed.

Introduction

The phase composition of the iron−nitrogen−hydrogen system is very well-known.[1−3] As a result of the reaction between iron and ammonia, iron nitrides are formed (γ'-Fe_4N, ϵ-Fe_3N, ζ-Fe_2N). Ammonia, hydrogen and nitrogen interactions with iron surface were analyzed in depth from the point of view of studying the elementary steps of catalytic ammonia synthesis as defined by Ertl's and Somorjai's researchers group and as described in reference papers.[4,5]

Nanocrystalline iron nitriding process can be regarded as an example of a system of parallel reactions, where, apart from iron nitriding reaction, catalytic ammonia decomposition also proceeds. During a nanocrystalline iron (A) nitriding reaction with ammonia (B), solid (C) as well as gaseous (D) products are formed. At the same time, catalytic ammonia decomposition takes place while nanocrystalline iron and iron nitrides are the catalyst of this reaction. Gaseous products (D, E) are formed.

The above-mentioned parallel reactions, generally, can be described according to the following scheme:

$$A + B \xrightarrow{k} C + D$$

$$B \xrightarrow{A,C,k_A,k_C} D + E$$

Three parallel chemical reactions between solid and gaseous substrate result in the formation of solid and gaseous products. Additionally, solid substrate A and solid product C are the catalyst of a reaction taking place in the gas phase. The reaction rate equations concerning particular constituents can be given as follows:

$$-\frac{dX_B}{dt} = k(T)f(X_B)f(X_A) + k_A(T)f(X_B) + k_C(T)f(X_B) \quad (1)$$

$$\frac{dX_C}{dt} = k(T)f(X_B)f(X_A) \quad (2)$$

$$\frac{dX_D}{dt} = k(T)f(X_B)f(X_A) + k_A(T)f(X_B) + k_C(T)f(X_B) \quad (3)$$

$$\frac{dX_E}{dt} = k_A(T)f(X_B) + k_C(T)f(X_B) \quad (4)$$

where X = concentration, $f(X)$ = concentration function, k = reaction rate constant, t = time, T = temperature, and subscripts A, B, C, D, and E refer to substances A, B, C, D, and E, respectively.

While studying the nitriding process of thin iron foils, Grabke[6,7] observed that the surface chemical reaction is the rate limiting step only in the initial stage of the process. The influence of diffusion through the product layer in case of nanocrystalline iron nitriding can be neglected.[8] It implies that there is no nitrogen concentration gradient in the iron nanocrystallites. Dissociative adsorption of ammonia is the rate limiting step during the whole iron nitriding process.

When the equilibrium state between the gas and solid phases is reached, it is only the effect of catalytic ammonia decomposition reaction on iron saturated with nitrogen and/or iron nitrides which can be measured. In this regard nitrogen contents of created nitrides depend on temperature and gaseous phase ammonia concentrations.[8,9] However, while the stationary state is present, three reactions i.e. nitrides formation and ammonia decomposition on iron and/or iron nitrides take place. Then, concentrations of reactants present in the gas phase change as a result of the conducted chemical reactions. Thus, in order to perform kinetics analysis of a considered system, besides specifying the solid mass changes, it is necessary to evaluate the composition of reacting gases. Such an analysis can be performed using a differential reactor with thermogravimetric (TG) measurement combined with continuous gas phase composition measurement. By applying experimental conditions (a lack of temperature gradient in the bed of solid, mixing of reactants in a gas stream, a lack of concentration gradient in the interface between phases as well as in the bulk of phases[10,11] so that the process is conducted in the kinetic region) one can directly obtain the reaction rate values.

Experimental Methods

The analyzed iron was obtained by fusion of magnetite with structured promoters of iron - calcium oxide (2.8%) and

* Corresponding author. Telephone: +48 91 449 47 30. Fax +48 91 449 46 86. E-mail address: rpelka@ps.pl.

10.1021/jp8079759 CCC: $40.75
Published on Web 12/16/2008

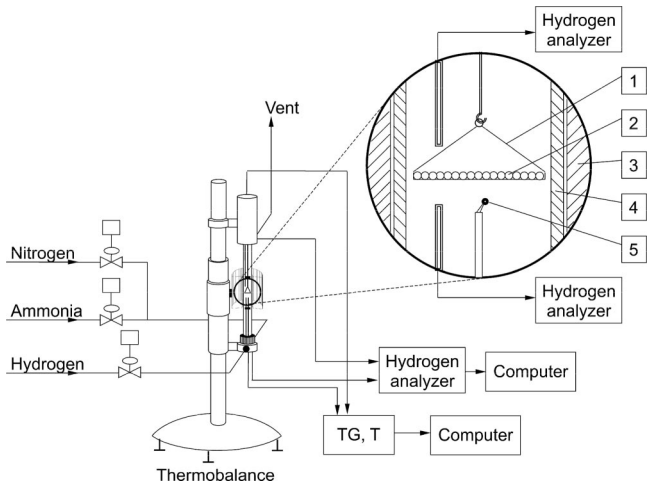

Figure 1. Experimental equipment: 1, sample holder; 2, single layer of grains; 3, reactor furnace; 4, reactor wall; 5, thermocouple.

aluminum oxide (3.3%). Then, the alloy was crushed and a fraction of grains of the size in the range 1.0−1.2 mm was separated. The reduction process of the alloy was performed stepwise from the temperature of 623 K (2 h), then 673 K (4 h), 723 K (24 h), and finally 773 K (24 h) at pure hydrogen load (99.999%) 10 $dm^3\ g^{-1}\ h^{-1}$, under atmospheric pressure. Then, the sample was overheated at 1073 K for 5 h. The material obtained in such a way contained iron nanocrystallites of a mean size 42 nm (determined by means of XRD method). The specific surface area determined by means of BET method (a method for surface area determination based on Brunauer−Emmet−Teller theory) was 5.5 m^2/g.

In order to perform investigations of the kinetics of parallel nanocrystalline iron nitriding and catalytic ammonia decomposition reactions an analytical system equipped with a flow tubular reactor was used (Figure 1). The system made it possible to conduct continuous thermogravimetric measurements combined with analyses of gas phase compositions. The reactor's construction enabled one to perform processes under aggressive conditions by means of applying special construction elements resistant to high temperature and gases such as ammonia. The flow rates of the applied gases, i.e., hydrogen, ammonia, and nitrogen, were determined by means of mass flow controllers. Hydrogen concentration in the reacting gas mixture was determined by means of an electronic system, based on a specific heat evaluation of gas mixture containing hydrogen and other gases. Gas samples were collected over and under a platinum basket containing a solid sample (Figure 1). The analytical system was made of materials resistant to aggressive chemical reagent. The experimental condition (temperature of measurement) was selected so that the value of heat conductivity was the same for nitrogen as that for ammonia. Thus, it is possible to specify hydrogen content in a gas phase. The mass and temperature of the analyzed solid samples as well as data concerning gas concentrations in the gas mixture were recorded digitally. In a platinum basket hanging on a balance arm the analyzed substance (ca. 1 g) was placed in a form of single layer of grains. The platinum from a sample holder did not affect the chemical processes taking place in the reactor. Measurements for a system without chemical reactions were performed. The reactor was filled in with nitrogen until all air was entirely removed. Then, the reactor's content was heated to 473 K, nitrogen flow was turned off and hydrogen flow was turned on (9 dm^3/h). Gas phase composition changes vs time were determined.

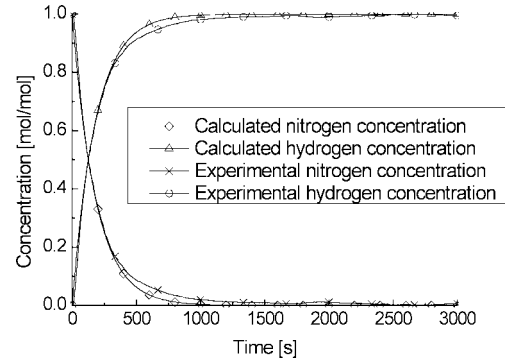

Figure 2. Gas phase composition changes. System without chemical reaction.

Nitriding processes were conducted under pure ammonia atmosphere at isothermal conditions, at various temperatures in the range of 623−723 K at ammonia load 500 $cm^3\ min^{-1}\ g_{mat}{}^{-1}$ until the analyzed sample's mass was stable, which could be seen on thermogravimetric (TG) curves as horizontal lines. The reacting gas mixture composition was determined. Gas samples were collected directly over the catalytic bed.

Results and Discussion

The results of the gas phase composition measurements performed over and under the solid bed during nitriding process prove, that a mixing of the components of the reacting gas mixture occurs in the reactor. It is due to an intensive convection.

The modeling of the gas phase composition changes, observed without any chemical reaction, was performed, basing on the mass balance of a reactor with an ideal mixing

$$\frac{dX}{dt} = \frac{\upsilon(X_i - X)}{n} \tag{5}$$

and after integration

$$X = X_i\left[1 - \exp\left(-\frac{\upsilon}{n}t\right)\right] \tag{6}$$

where n = total number of moles, υ = total molar flow rate, and subscript i refers to the feed stream.

A comparison of the calculated and experimental data, concerning hydrogen and nitrogen concentrations in the system without chemical reaction (N_2 and H_2 were introduced into the reactor one after the other), is presented in Figure 2. The experimental and calculated concentration values enabled one to determine the effective reactor volume which was 250 cm^3. The accordance of experimental gas composition data with the calculated data makes it possible to assume, that in the effective reactor volume an almost ideal mixing occurs under the experimental conditions.

The steady values of conversion degree of ammonia during catalytic ammonia decomposition reaction with all the applied grain diameters at lower temperature (724 K) (Figure 3) show that at this temperature the process was conducted in the kinetic reaction region, and that any internal diffusion effects could be neglected. At a higher temperature (773 K) an internal diffusion effect was observed only at grain diameters greater than 1.6 mm. It implies, that at grain diameters (1.0−1.2 mm) selected for further consideration the internal diffusion effects do not influence the catalytic ammonia decomposition reaction and nitriding reaction at all the experimental temperatures. Therefore, the applied reactor could be regarded as a differential one.

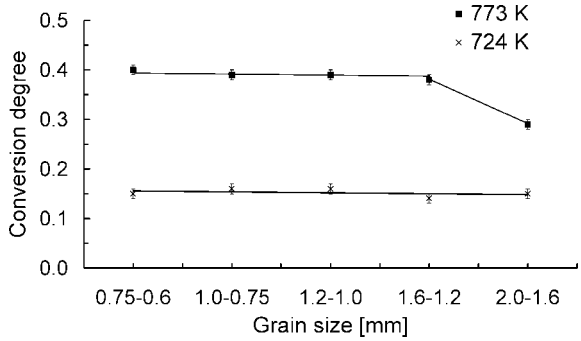

Figure 3. Ammonia conversion degree vs grain size.

Ammonia concentration changes observed in the reacting gas mixture are due to a physical mixing process proceeding between ammonia feeding the reactor and products of nitriding reaction and ammonia catalytic decomposition reaction. Ammonia is also consumed during the chemical processes mentioned above. Thus, the nitriding process's rate, and so the rate of nitriding reaction and the rate of simultaneously proceeding catalytic ammonia decomposition reaction, taking into account gas mixing process, can be described by an expression derived from Equation (1):

$$\frac{\mathrm{d}X_{\mathrm{NH3}}^{\mathrm{n+d}}}{\mathrm{d}t} = \frac{v(X_{\mathrm{NH3,i}} - X_{\mathrm{NH3}}^{\mathrm{c}})}{n} - k_{\mathrm{n}}(T)f(X_{\mathrm{NH3}}) - k_{\mathrm{d}}(T)f(X_{\mathrm{NH3}}) \tag{7}$$

where the following are denoted: d refers to a catalytic ammonia decomposition reaction; i refers to a feed stream; n refers to a nitriding reaction; NH3 refers to ammonia; superscripts n + d refer to a nitriding process (nitriding + ammonia decomposition reaction); and superscript c refers to calculated values without a chemical reaction.

The first item of the right side of the above equation corresponds to a mixing and gas exchange process in the reactor. Nevertheless, the second and the third items represent the nitriding reaction rate and ammonia catalytic decomposition reaction rates, respectively.

A solid sample mass gain, observed as TG curves, corresponds to an increase of nitrogen concentration in iron.

An iron nitriding process caused a change of gas phase composition, which was recorded against the background of physical mixing and gas exchange processes taking place in the reactor. Hydrogen concentration in the reaction volume, $X_{\mathrm{H2}}^{\mathrm{n+d}}$, was directly determined. The concentration changes resulted from ammonia load feeding the reactor as well as from nitriding reaction and catalytic ammonia decomposition reaction taking place in the reactor.

The results of the selected experiments are presented in the form of TG curves (Figure 4a) and hydrogen concentration changes (Figure 4b). The mass gain reached its maximal value and remained unchanged at every temperature for a twice longer time than that shown in Figure 4a, despite prolonged exposure to the nitriding atmosphere. As a result of the reaction, various iron nitrides were formed viz. γ'-Fe_4N, ϵ-$Fe_{3-2}N$. One inflection point on the obtained TG curves, corresponded to a phase transition between α-Fe(N) and γ'-Fe_4N. At this point two phases (α-Fe(N) and γ'-Fe_4N) exist simultaneously. The inflection point always appears below the stoichiometric concentration of nitrogen in γ'-Fe_4N. Moreover, the lower temperature the later the inflection point occurs and at a lower nitrogen concentration in a solid sample. This is because the nitriding reaction runs slower at lower temperatures—the inflection point occurs later in time—but ammonia concentration needed to start the formation of a new phase, richer in nitrogen, is reached when the nitrogen content in iron is lower—the inflection point occurs at lower and lower nitrogen concentrations in iron.

The hydrogen concentration in stationary states increased with temperature (Figure 4b). At temperatures greater than 673 K, it was possible to measure some amount of hydrogen even when the nitriding reaction was finished. It implied that the catalytic ammonia decomposition reaction took place on the iron surface.[9] Therefore, a decrease of ammonia concentration observed in a stationary state resulted only from a catalytic ammonia decomposition reaction.

On the basis of thermogravimetric analyses DTG curves were obtained (Figure 5), informing about the nitriding reaction rate. DTG curves also provide information about the amount of hydrogen resulting only from the nitriding reaction.

In order to determine the values of ammonia decomposition reaction rate the following algorithm was applied. Two temperatures were used as an example, namely 673 and 723 K. Initially, one calculated values of concentration occurring while hydrogen was replaced by ammonia without chemical reaction inside the reactor, $X_{\mathrm{NH3}}^{\mathrm{c}}$, $X_{\mathrm{H2}}^{\mathrm{c}}$ (Figures 6 and 7)a and by means of mass balance of stirred tubular reactor (eq 6) one can write:

$$\frac{\mathrm{d}X_{\mathrm{NH3}}^{\mathrm{c}}}{\mathrm{d}t} = \frac{v(X_{\mathrm{NH3,i}} - X_{\mathrm{NH3}}^{\mathrm{c}})}{n} \tag{8}$$

Then, using calculated curves of ammonia and hydrogen concentration changes, respectively, without chemical reaction as well as applying DTG curves, the gas phase composition was calculated, which could be observed, only if a nitriding reaction took place in the system, $X_{\mathrm{NH3}}^{\mathrm{n}}$, $X_{\mathrm{H2}}^{\mathrm{n}}$ (Figure 6.a) and 7.a)). It can be written as follows:

$$\frac{\mathrm{d}X_{\mathrm{NH3}}^{\mathrm{n}}}{\mathrm{d}t} = \frac{v(X_{\mathrm{NH3,i}} - X_{\mathrm{NH3}}^{\mathrm{c}})}{n} - k_{\mathrm{n}}(T)f(X_{\mathrm{NH3}}) \tag{9}$$

Comparing results of hydrogen concentration measurement - aggregating influence of nitriding reaction and catalytic ammonia decomposition reaction, $X_{\mathrm{H2}}^{\mathrm{n+d}}$ (Figures 6b and 7b)—with the results of calculations concerning hydrogen content in the reaction mixture for nitriding reaction, $X_{\mathrm{H2}}^{\mathrm{n}}$, the amount of hydrogen was calculated, which was generated as a result of catalytic ammonia decomposition reaction—dashed area in Figures 6b and 7b. According to catalytic ammonia decomposition reaction stoichiometry, the amount of nitrogen, $X_{\mathrm{N2}}^{\mathrm{d}}$ (Figure 6b and 7b) is 3-fold lower than the amount of hydrogen generated during catalytic ammonia decomposition reaction, $(X_{\mathrm{H2}}^{\mathrm{n+d}} - X_{\mathrm{H2}}^{\mathrm{n}})$. Then, the amount of ammonia remaining in the reactor after nitriding reaction, $X_{\mathrm{NH3}}^{\mathrm{n}}$, was decreased by hydrogen and nitrogen amounts which were generated during catalytic ammonia decomposition process, namely by the amount $(X_{\mathrm{H2}}^{\mathrm{n+d}} - X_{\mathrm{H2}}^{\mathrm{n}})$ and $X_{\mathrm{N2}}^{\mathrm{d}}$ respectively. Thus, ammonia concentration changes occurring during nanocrystalline iron nitriding process were determined, $X_{\mathrm{NH3}}^{\mathrm{n+d}}$, (Figure 6b and 7b). The difference between concentrations $X_{\mathrm{NH3}}^{\mathrm{n}}$ and $X_{\mathrm{NH3}}^{\mathrm{n+d}}$ results from catalytic ammonia decomposition reaction. On the basis of eq 7, the following relation can be written:

$$k_{\mathrm{d}}(T)f(X_{\mathrm{NH3}}) = \frac{v(X_{\mathrm{NH3,i}} - X_{\mathrm{NH3}}^{\mathrm{c}})}{n} - k_{\mathrm{n}}(T)f(X_{\mathrm{NH3}}) - \frac{\mathrm{d}X_{\mathrm{NH3}}^{\mathrm{n+d}}}{\mathrm{d}t} \tag{10}$$

However, the observed decrease of ammonia concentration was influenced by a decrease of ammonia amount because

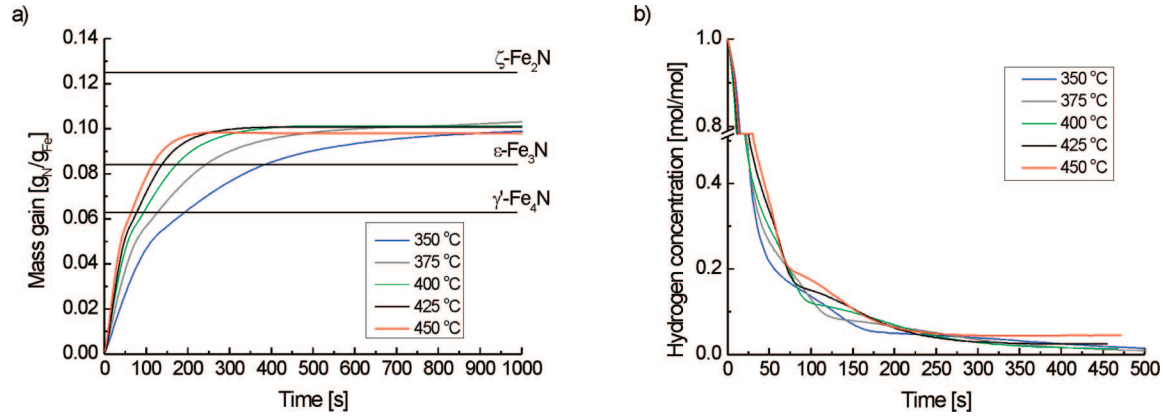

Figure 4. (a) TG curves for nitriding process of nanocrystaline iron. (b) Gas phase composition changes—nitriding process.

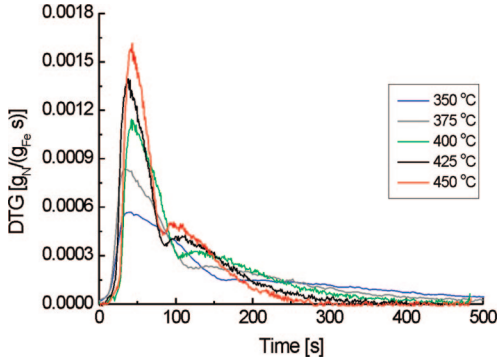

Figure 5. DTG curves for nitriding process of nanocrystaline iron.

of catalytic decomposition reaction as well as by an increase of reactant volume because of hydrogen and nitrogen formation, which on account of gas phase mixing caused ammonia dilution. Hence, making use of the determined concentrations of particular gas phase components, the amount of ammonia amount which really was decomposed at any moment was determined.

Figures 8 and 9 present the results in the form of DTG, regarding nitriding reaction, as well as calculated values of ammonia decomposition reaction rate for temperatures 673 and 723 K respectively. Initially, (A region) ammonia replaced hydrogen inside the reactor. One could observe only catalytic ammonia decomposition. The rate of this reaction increased on α-Fe, because surface nitrogen concentration increased. The rate of this reaction reached its maximum value at the moment when nitriding reaction just started. Also, the iron bulk concentration of nitrogen became higher and higher till the critical bulk concentration was achieved. Nitrogen solution in iron was obtained. Nitriding reaction (B region) started after a minimal concentration of ammonia needed for nitriding reaction to be commenced, equal to ca. 0.3 mol NH_3/mol, was reached. After the phase transition of smaller nanocrystallites, the nitriding process took place on two phases - α-Fe(N) and γ'-Fe_4N. Nitrogen concentration on γ'-Fe_4N surface was very low in comparison to surface nitrogen concentration on α-Fe phase. Thus, while the surface of α-Fe decreased, the total surface nitrogen concentration decreased, and ammonia decomposition rate decreased as well. Before the phase transformation of α-Fe(N) to γ'-Fe_4N was almost completed, the nitriding reaction slowed down and its rate reached its minimum value. At this moment ammonia decomposition reaction rate was nearly 0. An increase in the rates of both reactions was observed after a complete phase transformation. Nevertheless, nitriding reaction rate quickly reached the next maximum, and then stabilization of nitriding reaction rate took place (C region). Then, nitriding reaction rate went down, but ammonia catalytic decomposition, after reaching the next maximum value, reached a stable state. Only catalytic ammonia decomposition reaction determined the gas phase composition after stationary state was reached, viz., when the nitriding reaction was completed. The participation of catalytic ammonia decomposition reaction in the entire nitriding process is the higher the higher process temperature is maintained.

In Figure 10, the sum of rates of the nitriding reaction and ammonia decomposition is presented.

Considering nanomaterials, a diffusion in the bulk can be neglected. It implies, that the surface chemical reaction can be

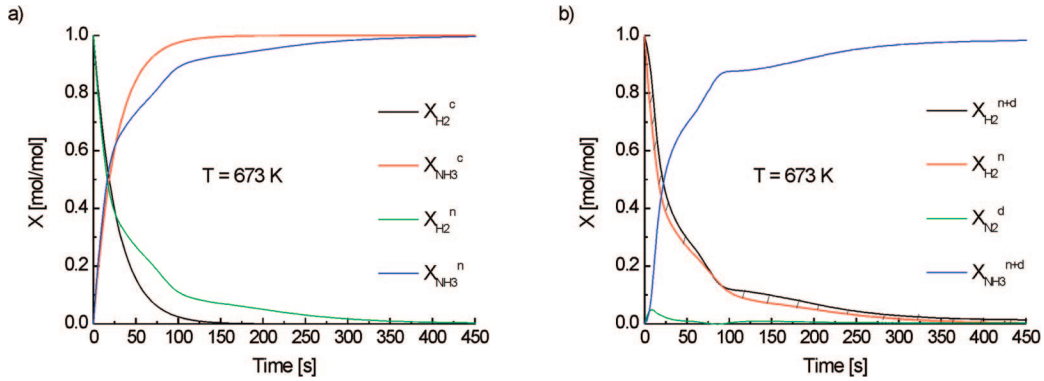

Figure 6. Gas phase composition changes at 673 K: (a) calculated concentrations values and nitriding reaction; (b) gas phase composition occurring during nitriding process.

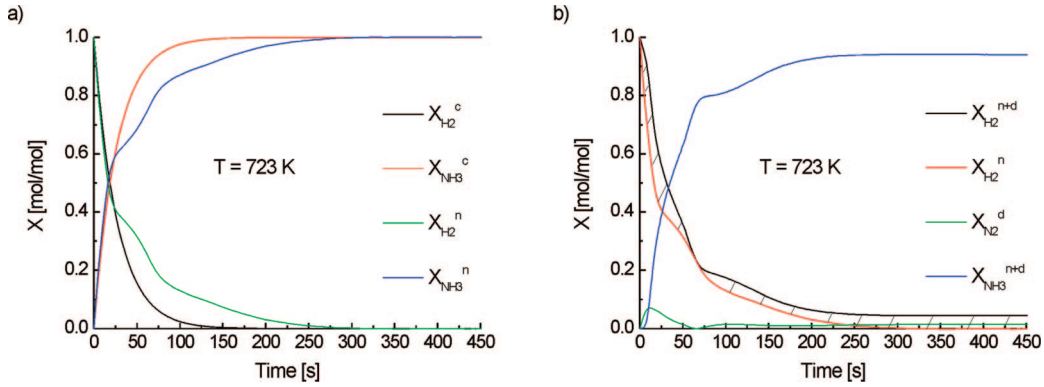

Figure 7. Gas phase composition changes at 723 K: (a) calculated concentrations values and nitriding reaction; (b) gas phase composition occurring during nitriding process.

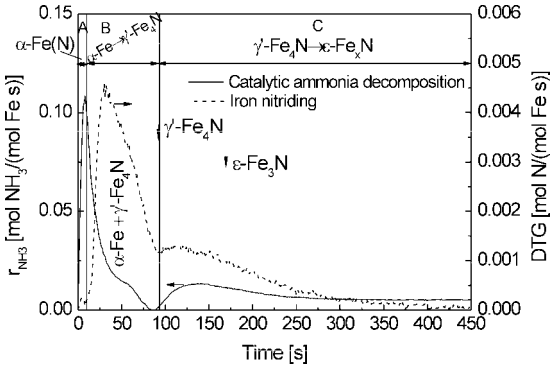

Figure 8. Reaction rates at 673 K—nitriding reaction (DTG) and catalytic ammonia decomposition reaction (r_{NH3}).

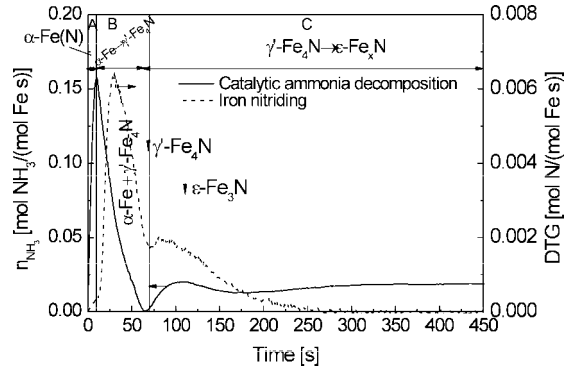

Figure 9. Reaction rates at 723 K—nitriding reaction (DTG) and catalytic ammonia decomposition reaction (r_{NH3}).

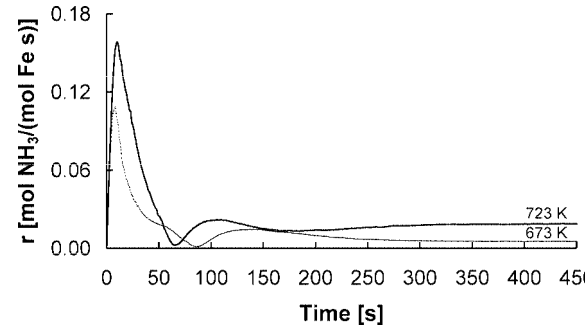

Figure 10. The rate of nitriding process (nitriding reaction and ammonia decomposition) at temperature 673 and 723 K.

the rate limiting step. Then, between reactants on the surface and dissolved in the bulk the thermodynamic equilibrium holds. The relationship between the concentration of nitrogen in iron bulk, X_b, and the surface coverage degree, θ, is described by the McLean-Langmuir equation:[12]

$$\frac{\theta}{1-\theta} = \frac{X_b}{1-X_b}\exp\left(-\frac{\Delta G}{RT}\right) \qquad (11)$$

where ΔG = free Gibbs enthalpy of segregation, R = gas constant, and T = temperature.

Considering the critical point between α-Fe(N) and γ'-Fe_4N phase and assuming, that for α-Fe phase $\Delta G = -110$ kJ/mol[13] and $X_b = 0.0012$ mol/mol,[2] it was calculated that $\theta = 0.999998$ at temperature 673 K. At this point the rate of nitriding reaction was 0. Thus we have the Langmuir equation[14]

$$r = pk_{NH3,ads}S(1-\theta) - k_{NH3,dec}S\theta^2 \text{ [mol/s]} \qquad (12)$$

where p = gas partial pressure, k_{ads} = adsorption constant, $k_{NH3,dec}$ = ammonia decomposition constant, and S = total surface area, can be transformed as follows:

$$pk_{NH3,ads}(1-\theta) = k_{NH3,dec}\theta^2 \text{ [mol/s]} \qquad (13)$$

Taking into account that $\theta = 0.999998$ and $p = 0.297$ bar, one can obtain

$$\frac{k_{NH3,ads}}{k_{NH3,dec}} = 1683500\frac{1}{\text{bar}} \qquad (14)$$

From Figure 8, for 1 g of solid sample, it is known that $k_{NH3,dec}$ S $\theta^2 = 0.00162$ mol/s. Assuming, that S = 5.5 m^2/g, it was calculated that the value of $k_{NH3,dec} = 0.00029$ mol g m^{-2} s^{-1} and then $k_{NH3,ads} = 2685$ mol bar^{-1} s^{-1}.

The number of collisions can be described as follows:

$$z = \frac{1}{N}\frac{p}{\sqrt{2\,\pi\,m\,k\,T}}\left[\frac{\text{mol}}{m^2 s}\right] \qquad (15)$$

Here N = Avogadro's number, m = mass of particle hitting the surface, and k = the Boltzmann constant.

It was found that at the critical point $z = 1230$ mol m^{-2} s^{-1}. The number of collisions resulting from the total surface area (S = 5.5 m^2/g) and mass of the solid sample (1 g) used during the investigations was $z' = 6765$ mol s^{-1}. Thus the sticking coefficient, s_0, for $\theta = 0$ is 0.12. The corresponding literature values are $s_0 = 0.16$ on the Fe(100) surface at −153 °C[15] and 0.03 for Fe(111) surface contaminated with oxygen at 27 °C.[16]

The above presented calculations were carried out assuming that the whole surface of the solid sample took part in the nitriding process. However one should take into consideration that only ca. 50% of the whole surface is available for gas reactants.[17,18]

Conclusions

A combination of thermogravimetric measurement of mass changes of solid samples, during reaction between nanocrystalline iron and ammonia, with gas phase composition analysis makes it possible to estimate rates of parallel reactions at any moment of the investigated process.

The obtained results concerning catalytic ammonia decomposition reaction rate imply, that when nanocrystalline iron nitriding process is conducted one can observe reaction rate changes of nitriding reaction as well as of catalytic ammonia decomposition reaction vs time. Nitriding reaction rate reaches the highest value during α-Fe nitriding reaction. Catalytic ammonia decomposition reaction rate reaches the highest value upon α-Fe as well, although the reaction rate values of this reaction are clearly lower upon recently created nitrides. This is due to lower nitrogen concentration on the iron nitride surface in comparison to nitrogen concentration on iron surface.

On the basis of the calculations performed for the critical point between α-Fe and γ'-Fe_4N phases, the rate constants of ammonia decomposition and ammonia adsorption process were estimated. The number of collisions and the sticking coefficient were also assessed.

Acknowledgment. The work has been financed as Research Project No. NN 507 4461 33.

References and Notes

(1) Lehrer, E. *Z. Elektrochem.* **1930**, *36* (6), 383–392.
(2) Kunze, J. *Nitrogen and Carbon in Iron and Steel—Thermodynamics*; Physical Research Volume 16; Akademie Verlag: Berlin, 1990.
(3) Kooi, B. J.; Somers, M. A. J.; Mittemeijer, E. J. *Metall. Mater. Trans. A* **1996**, *27 A*, 1064.
(4) Jennings, J. R., Ed.; *Catalytic Ammonia Synthesis*; Plenum Press, New York, 1991,
(5) Aika, K.; Christiansen, L. J.; Dybkjaer, I.; Hansen, J. B.; Nielsen, P. E. H.; Nielsen, A.; Stolze, P.; Tamaru, K. *Ammonia Catalysis and Manufacture*; Springer Verlag, Berlin/Heidelberg, 1995.
(6) Grabke, H. J. *Ber. Bunsen-Ges. Phys. Chem.* **1968**, *4*, 533–543.
(7) Grabke, H. J. *Arch. Eisenhüttenwesen* **1973**, *44*, 603–608, no. 8.
(8) Wróbel, R.; Arabczyk, W. *J. Phys. Chem. A* **2006**, *110*, 9219–9224.
(9) Arabczyk, W.; Zamynny, J. *Catal. Lett.* **1999**, *60*, 167.
(10) Baranski, A.; Dziembaj, R.; Kotarba, A.; Jagan, J. M.; Jojewska, J.; Pieprzyk, E.; Baerns, M.; Mleczko, L. *Solid State Ionics* **1997**, *101—103*, 677–680.
(11) Perego, C.; Peratello, S. *Catal. Today* **1999**, *52*, 133–145.
(12) Benard, J. *Stud. Surf. Sci. Catal.* **1983**, *13*, 261.
(13) Grabke, H. J. *Z. Phys. Chem. Neue Folge* **1976**, *100*, 185.
(14) Langmuir, I. *J. Am. Chem. Soc.* **1918**, *40*, 1361.
(15) Weiss, M.; Ertl, G.; Nietsche, F. *Appl. Surf. Sci.* **1979**, *2*, 614.
(16) Gay, I. D.; Textor, M.; Mason, R.; Iwasawa, Y. *Proc. R. Soc. (London)* **1977**, *A356*, 25.
(17) Arabczyk, W.; Narkiewicz, U.; Moszynski, D. *Appl. Catal. A: Gen.* **1999**, *182*, 379.
(18) Boisen, A.; Dahl, S.; Norskov, J. K.; Christensen, C. H. *J. Catal.* **2005**, *230*, 309–312.

JP8079759